Available online at www.sciencedirect.com

SciVerse ScienceDirect

Procedia Engineering 19 (2011) 306 – 311

Procedia Engineering

www.elsevier.com/locate/procedia

1st CIRP Conference on Surface Integrity (CSI)

Numerical Analysis of the Influence of Johnson-Cook-Material Parameters on the Surface Integrity of Ti-6Al-4V

V. Schulze[a] and F. Zanger [a]*

[a]*Karlsruhe Institute of Technology (KIT), wbk Institute of Production Science, Kaiserstraße 12, 76131 Karlsruhe, Germany*

Abstract

During machining metals the material of the work piece is highly deformed and heated, which influences surface integrity. To simulate the machining process the thermo-mechanical material behavior in dependence of strain, strain rate and temperature has to be well known. One of the most used material models is the Johnson-Cook-Model, where the material dependent parameters are determined by Split-Hopkinson pressure bar tests. For the titanium alloy Ti-6Al-4V used for the simulations different investigations with the goal of determining material parameters have been published. However, the presented results vary significantly. It is expected that these varying parameters result in different predictions of surface integrity after machining. This influence is investigated by machining simulations using a self-developed continuous remeshing method.

Selection and peer-review under responsibility of Prof. E. Brinksmeier

Keywords: Machining, Finite element method (FEM), Surface integrity

1. Introduction

For simulating machining processes it is important to model the material behavior of the work piece. At machining Ti-6Al-4V segmented chips are formed, which are difficult to predict using FEM. Therefore a lot of research has been done in this field [1-5]. One of the most often used material models is the Johnson-Cook-Model [6], which describes the yield stress in dependence of the plastic strain, plastic strain rate and temperature. To use this model for a special work piece material the material dependent constants have to be determined. For Ti-6Al-4V a lot of researchers determined these constants using compression tests by means of a split-Hopkinson pressure bar to use them for FEM simulations [7-10]. Although they did their analyses for the same material, there are some differences within the material

* Corresponding author. Tel.: +49-721-608-42450; fax: +49-721-608-45004
E-mail address: frederik.zanger@kit.edu

1877-7058
doi:10.1016/j.proeng.2011.11.117

specific constants. That implies different results in terms of forces, temperatures and chip shapes when using these differing constants for machining simulation. Furthermore, the changed material behavior influences the resulting surface integrity.

2. Simulation Model

To investigate the influence of differing material parameters on surface integrity after machining a FEM simulation model was built up, which is suited for the calculation of surface integrity caused by mechanical and thermal tool loads during the metal-cutting of Ti-6Al-4V. The cutting tool has to be in full contact with the work piece and chip during the whole simulation time. Thus it was necessary to carry out the numerical investigations with a self-developed continuous remeshing method using ABAQUS, where a new mesh was created for the whole work piece every 5 µm of relative displacement between the tool and work piece to avoid strong distortion of elements, see Fig. 1. This mesh was created with different element densities, so that the shear zones and resulting surface could be simulated with a high resolution. The smallest element edge length was $e_x=2.5\ \mu m$. The work piece and the tool were modeled thermo-mechanically coupled using elements of the type 'CPE4T' out of the element library of ABAQUS [11]. At the beginning of each simulation the work piece was meshed by approximately 16000 elements. The number of elements was increasing up to about 25000 elements during the simulations. The specific heat capacity c_p of the tool and its heat transfer to the surrounding were adapted as shown in [12]. Due to this proceeding, constant temperatures were reached after a length of cut which was three times the uncut chip thickness. After the chip was created the tool was lifted from the surface in order to mechanically relax and cool down the work piece to room temperature, see Fig. 1.

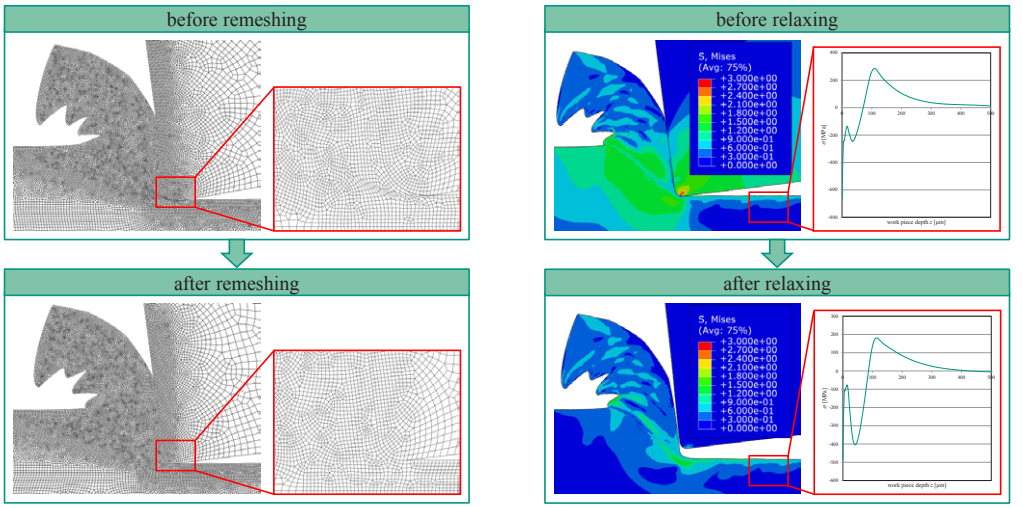

Fig. 1: (a) Continuous remeshing, (b) relaxing and cooling down the work piece.

With this simulation model it is possible to calculate the residual stress states as well as established parameters like process forces, cutting temperatures and chip shapes during the metal-cutting of materials which tend to form segmented chips. The process parameters that were varied are the cutting velocity ($v_{c1,S}=100\ m/min$, $v_{c2}=200\ m/min$, $v_{c3}=300\ m/min$) and the uncut chip thickness ($h_{1,S}=100\ \mu m$, $h_2=200\ \mu m$, $h_3=300\ \mu m$). The geometry of the cutting tool was varied in terms of the clearance angle ($\alpha_{1,S}=7°$, $\alpha_2=5°$, $\alpha_3=10°$), the rake angle ($\gamma_1=7°$, $\gamma_2=-5°$, $\gamma_{3,S}=-7°$, $\gamma_4=-10°$) and the cutting edge radius ($r_{\beta 1}=15\ \mu m$, $r_{\beta 2,S}=30\ \mu m$, $r_{\beta 3}=45\ \mu m$). The standard parameters are indexed by an additional 's'.

3. Material Model

The thermo-physical material parameters used for the work piece and tool were taken from [13, 14] and are compiled in Table 1. The inelastic heat fraction describes the percentage of the plastic work being converted into heat.

Table 1: Thermo-physical material parameters.

Material parameters	Units	work piece	tool
Young's modulus E	[GPa]	115	210
Density ρ	[g/cm³]	4.43	11.9
heat conductivity λ	[W/(m·K)]	7.2	36.8
specific heat c_p	[J/(kg·K)]	505	400
thermal expansion α	[1/K]	8.9E-6	-
friction coefficient μ	[-]	0.15	
inelastic heat fraction η	[-]	0.9	

The applied material model for the work piece according to Johnson and Cook (JC) [11] can be divided into three multiplicative factors: $f(\varepsilon_{pl})$ describes increasing stresses with increasing plastic strains, $f(\dot{\varepsilon}_{pl})$ describes hardening due to increasing strain rates and $f(T)$, that describes the softening due to high temperatures. The JC yield stress σ_f can be calculated as:

$$\sigma_f = (A + B \cdot \bar{\varepsilon}_{pl}^{\,n}) \cdot \left[1 + C \cdot ln\left(\frac{\dot{\bar{\varepsilon}}_{pl}}{\dot{\varepsilon}_0} \right) \right] \cdot \left[1 - \left(\frac{T - T_t}{T_m - T_t} \right)^m \right] \qquad (1)$$

The coefficients A, B, C, n and m of the Johnson-Cook model describe characteristic material constants and are adjusted to experimental data, see Table 2. Although the parameters differ considerably in parts they were all determined for describing the material behavior of the same material, Ti-6Al-4V.

Table 2: Johnson-Cook material coefficients.

Material coefficients	Units	Lee and Lin (a) [7]	Lee and Lin (b) [8]	Shivpuri et al. [9]	Meyer and Kleponis [10]
A	[MPa]	782.7	724.7	870.0	896.0
B	[MPa]	498.4	683.1	990.0	656.0
C	[-]	0.028	0.035	0.011	0.0128
n	[-]	0.28	0.47	0.25	0.5
m	[-]	1.0	1.0	1.0	0.8

4. Residual Stress states

Ti-6Al-4V forms segmented chips for the whole range of cutting parameters. The segmentation influences the stress and strain states during machining, which, in turn, changes the residual stress states

periodically in dependence of the segment pitches. Because this influence is not measured during experiments, the residual stress states were identified for different positions behind the tool and the mean values were calculated, see Fig. 2. To compare the results of different simulations the averaged values were taken. Due to the strain rate hardening and temperature softening effects of Ti-6Al-4V compressive surface residual stresses remain after machining.

The resulting depth profiles can be characterized by a few characteristic points (Fig. 2). For the stress profiles these points are the maximum compressive and tensile residual stresses in cutting direction $\sigma^{II}_{p,\,max}$, $\sigma^{II}_{t,\,max}$, respectively and the depth of the compressive stresses $z\left(\sigma^{II}_{p}\right)$. The strain profile can be characterized by the maximum plastic strain $\varepsilon_{pl,max}$ and the depth of plastic deformation $z\left(\varepsilon_{pl}\right)$, that is determined by defining a lower limit $\varepsilon_{pl,lim} = 0.01$.

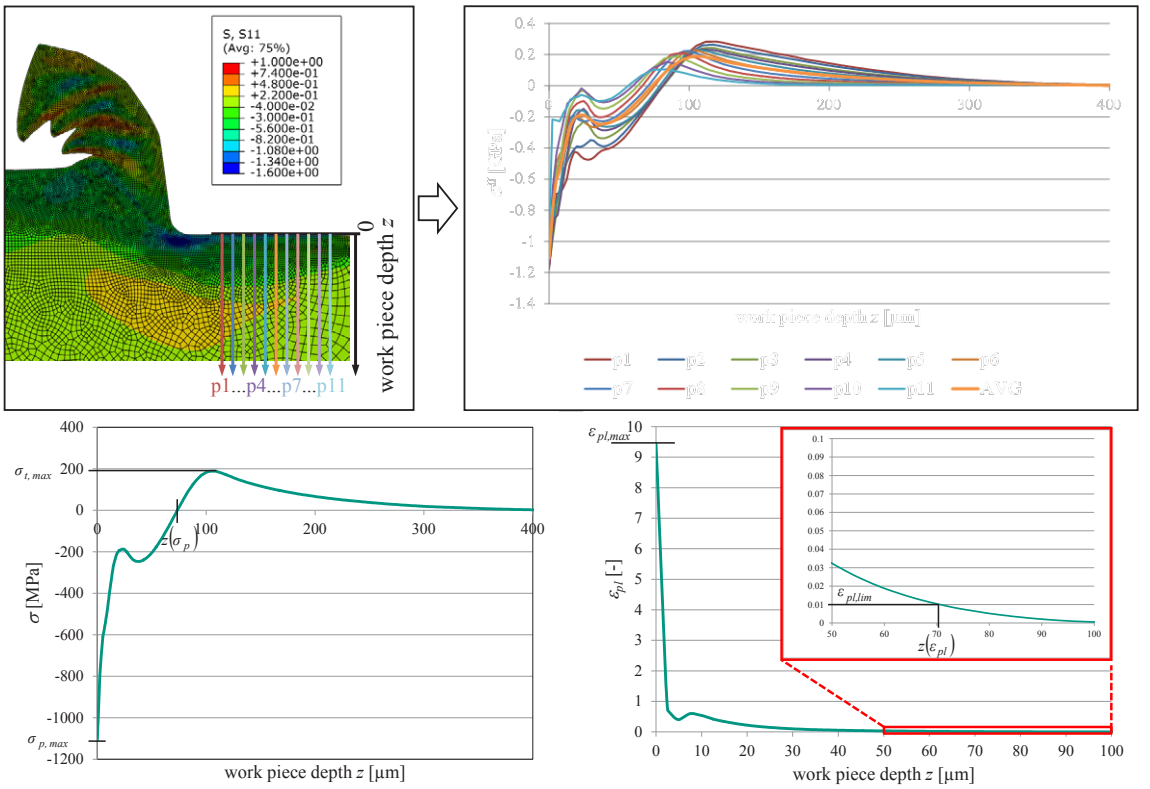

Fig. 2: Determination of the residual stress states and characterization of the depth profiles.

5. Influence on Surface Integrity

To clarify the influences of each factor of the material model they are first considered separately, see Fig. 3. The parameters according to Shivpuri et al. describe the highest strain and lowest strain rate influence of the four considered parameter sets, while the two different parameter sets according to Lee and Lin are characterized by the highest strain rate and lowest strain influence. The parameters of Meyer and Kleponis are characterized by the lowest elastic limit and the highest softening behavior with increasing temperatures. All the other models have the same temperature dependence that is less distinct.

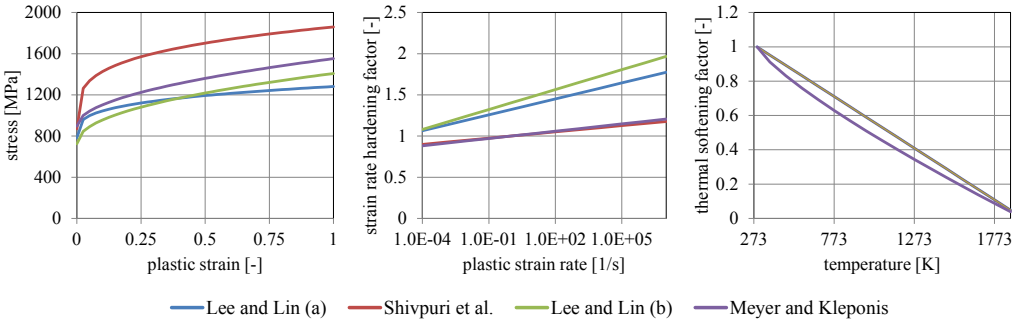

Fig. 3: Influence of the (a) plastic strain, (b) plastic strain rate, (c) temperature.

To show the influences of the investigated process, geometry and material parameters only the main results are summarized in terms of their influence on the surface characteristics they affect most significantly, see Fig. 4. Because the clearance angle α showed the smallest influence and no significant differences between the four material parameter sets, it is not illustrated.

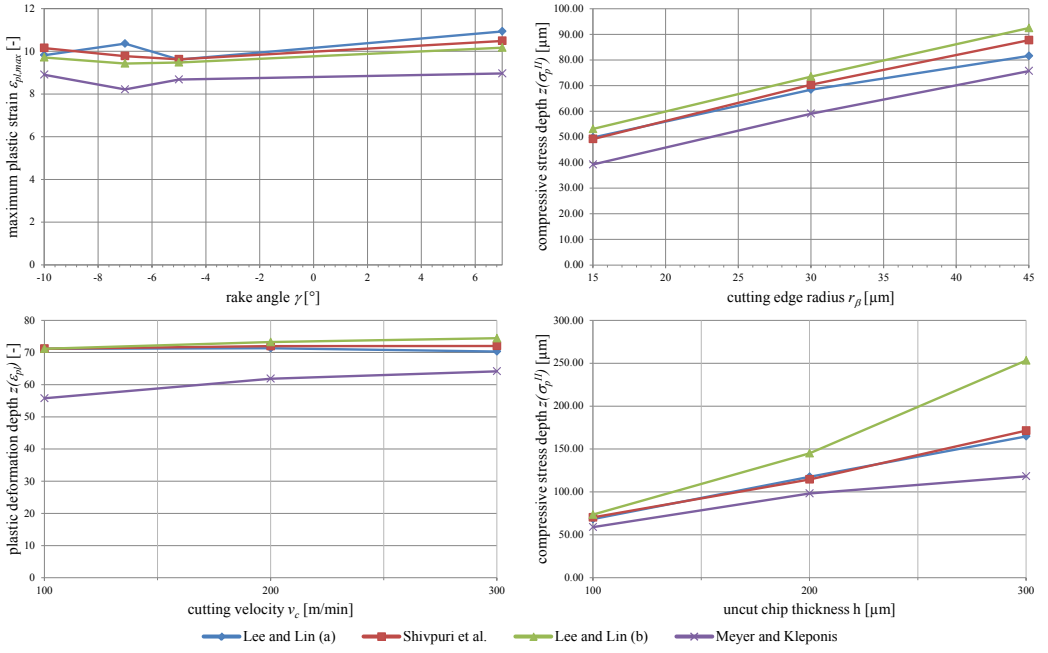

Fig. 4: Influence of the (a) rake angle γ, (b) cutting edge radius r_β, (c) cutting velocity v_c, (d) uncut chip thickness h.

The rake angle γ showed decreasing depths of compressive stress and depths of plastic deformation with increasing angles, whereas the maximum plastic strain showed a falling tendency within negative angles. With increasing cutting edge radius r_β the depth of compressive stress and plastic deformation increases. The maximum values of tensile stresses and plastic strains showed the same behavior. The depth of plastic deformation increases slightly within the varied range of cutting velocities. This is due to the growing plastic strain rate. The dominating influence of the plastic strain rate can also be seen when varying the uncut chip thickness, where an increase causes rising depth of compressive stresses.

The variation of the rake angle γ and cutting edge radius r_β showed the same behavior for all four material parameter sets that are considered. The results of the variation of the cutting velocity v_c showed two opposing mechanisms, the influence of temperature and strain rate. The depth of plastic deformation increased more sharply at the parameter set of Meyer and Kleponis, which is due to the higher temperature softening. The influence of the strain rate can be detected at the other parameter sets, where Lee and Lin (a) shows the highest influence. When varying the uncut chip thickness, the depths of compressive stresses show for the four parameter sets the same order as for the influence of the plastic strain rate (cf. Fig. 3).

6. Conclusion

The results showed that the simulation of influences on surface integrity depends on the Johnson-Cook material parameters. In this connection the clearance angle, the rake angle and the cutting edge radius have the smallest effect, while the cutting velocity and uncut chip thickness showed to be of higher interest. The used material parameter sets showed the same trends with one exception. In further steps the results have to be compared to experimental measurements to find out which material model is most suitable in combination with the used simulation model.

References

[1] Bäker M. An Investigation of the Chip Segmentation Process Using Finite Elements. *Technische Mechanik* 2003; **23-1**:1-9.

[2] Umbrello D. Finite element simulation of conventional and high speed machining of Ti6Al4V alloy. *Journal of Materials Processing Technology* 2008; **196**:79-87.

[3] Karpat, Y. Temperature dependent flow softening of titanium alloy Ti6Al4V: An investigation using finite element simulation of machining. *Journal of Materials Processing Technology* 2011; **211**:737-749.

[4] Sima M., Özel T. Modified material constitutive models for serrated chip formation simulations and experimental validation in machining of titanium alloy Ti-6Al-4V. *International Journal of Machine Tools & Manufacture* 2010; **50**:943-960.

[5] Özel T., Sima M. Srivastava A.K., Kaftanoglu B. Investigations on the effect of multi-layerd coated inserts in machining Ti-6Al-4V alloy with experiments and finite element simulations. *CIRP Annals - Manufacturing Technology* 2010; **59**:77-82.

[6] Johnson G., Cook W. Fracture Characteristics Of Three Metals Subjected To Various Strains, Strain Rates, Temperatures And Pressures. *Engineering Fracture Mechanics* 1985; **23**:31-48.

[7] Lee, W.-S., Lin, C.-F. High-temperature deformation behaviour of Ti6Al4V alloy evaluated by high strain-rate compression tests. *Journal of Materials Processing Technology* 1998; **75:**127–136.

[8] Lee, W.-S., Lin, C.-F. Plastic deformation and fracture behaviour of Ti–6Al–4V alloy loaded with high strain rate under various temperatures. *Materials Science and Engineering* 1998; **A241**:48–59.

[9] Shivpuri, R., Hua, J., Mittal, P., Srivastava, A.K., Lahoti, G.D. Microstructure-Mechanics Interactions in Modeling Chip Segmentation during Titanium Machining. *CIRP Annals - Manufacturing Technology* 2002, **51-1**:71-74.

[10] Meyer, H. W., Kleponis, D. S. Modeling the high strain rate behavior of titanium undergoing ballistic impact and penetration. *International Journal of Impact Engineering*, 2001; **26**:509-521.

[11] ABAQUS Analysis User's Manual, Version 6.10, 2011.

[12] Lorentzon J., Järvstråt N. Modelling tool wear in cemented-carbide machining alloy 718. *International Journal of Machine Tools & Manufacture* 2008; **48**:1072-1080.

[13] Obikawa, T., Shinozuka, J., Shriakashi, T. Analytical prediction of cutting performance of grooved rake face tools. *Bulletin of Japanese Society of Precision Engineering*, 1995; **61-9**:1295-1299.

[14] CES EduPack, 2010, Version 6.2.0, Granta Design Limited.